Generalized Approach for Prediction of Jet Grout Column Diameter

Shui-Long Shen[1]; Zhi-Feng Wang[2]; Jun Yang, M.ASCE[3]; and Chu-Eu Ho, M.ASCE[4]

Abstract: This paper presents a generalized approach for predicting the diameter of jet grout columns based on the theoretical framework of turbulent kinematic flow and soil erosion. The proposed calculation method is applicable to all conventional jet-grouting systems and takes into account the full range of operational parameters, fluid properties, soil strength, and particle size distribution, including the effect of the injection time on erosion distance. It was demonstrated that the increase in the jet grout column diameter arising from the use of a compressed air shroud in the double and triple fluid systems is approximately 27–81% for the typical range of air pressure of 0.5–1.5 MPa. The proposed method was applied to four case histories involving four variants of jet-grouting systems, i.e., single fluid, double fluid, triple fluid, and an enhanced triple fluid system. Comparison between the calculated and the measured jet grout column diameters indicated that the proposed method can produce reasonable predictions for a variety of soil conditions. It was shown that jet grout columns formed by the enhanced triple fluid system are larger than those formed by the conventional triple fluid system by approximately 36% on average. The proposed generalized approach allows all the key variables to be considered and is a useful means for the design of ground improvement by jet grouting. **DOI: 10.1061/(ASCE)GT.1943-5606.0000932.** *© 2013 American Society of Civil Engineers.*

CE Database subject headings: Soil stabilization; Jet grouting; Turbulent flow; Soil erosion; Predictions; Columns.

Author keywords: Ground improvement; Jet grouting; Turbulent flow; Soil erosion; Predictions; Columns.

Introduction

Soft ground improvement technologies based on chemical reactions, such as deep mixing (Han et al. 2002, 2007; Chai et al. 2005; Yin and Fang 2006; Shen et al. 2008; Chen et al. 2013; Horpibulsuk et al. 2012) and jet grouting (Burke 2004; Mihalis et al. 2004; Fang et al. 2006; Shen et al. 2009a, 2013a, b; Wang et al. 2013), are commonly adopted to enhance stability when infrastructures are constructed in soft deposits. Jet-grouting technology is based on the injection of high velocity fluids through small-diameter nozzles to erode the soil and mix it with injected grout to form a soil-cement column. Based on the different methods of fluid injection, jet-grouting technology can be classified as a (1) single fluid system (only grout), (2) double fluid system (grout and air), or (3) triple fluid system (water, grout, and air). In the double fluid system, the cutting distance is increased by introducing a compressed air shroud around the grout jet. In the triple fluid system, the cutting jet utilizes water instead of grout, which is also surrounded by a compressed air shroud, while the grout is injected separately through a nozzle located at a lower elevation at a much smaller pressure to mix with the eroded soil. In this case, the cutting distance is further enhanced because of the lower viscosity of water in comparison with that of grout. Tsujita (1996) introduced a variation of the conventional triple fluid system, herein termed the enhanced triple fluid system. In the enhanced triple fluid system, both the water and grout jets are simultaneously injected under high pressures (Shen et al. 2009b), such that the soil is subjected to two stages of erosion: initially by the water jet and then by secondary erosion by the grout jet. The exposure of the soil twice to the cutting action of the jets enables a larger column to be formed.

Although jet-grouting technology is continuously being developed in an attempt to increase the dimensions and strength of the jet grout columns, one problem that is still of great concern to the designers is the uncertainty associated with determining the diameter of the jet grout column at the design stage. The achievable column diameter is governed by the jetting parameters adopted and soil properties; hence, due consideration of these influencing factors is necessary for proper prediction of the column diameter. The existing methods for predicting the column diameter can be divided into two basic categories: (1) empirical approach (Shibazaki 2003; Mihalis et al. 2004) and (2) theoretical approach (Modoni et al. 2006; Ho 2007; Wang et al. 2012). The existing methods have been developed primarily for the single fluid system.

In this paper, the existing methods are briefly reviewed and discussed and a generalized method of predicting the diameter of the jet grout column for all three jet-grouting systems is introduced based on the theory of turbulent kinematic flow and soil erosion. In the proposed method, the operational parameters used in different jet-grouting systems, such as the number of nozzles, diameter of nozzles, flow rate, jetting pressure, withdrawal rate, and rotating speed, as well as the in situ soil properties, such as soil strength and particle size distribution, are considered. The predicted column diameters are compared with field measurements obtained from four full-scale trials.

[1]Professor, Dept. of Civil Engineering, Shanghai Jiao Tong Univ., and State Key Laboratory of Ocean Engineering, Shanghai 200240, China (corresponding author). E-mail: slshen@sjtu.edu.cn

[2]Ph.D. Student, Dept. of Civil Engineering, Shanghai Jiao Tong Univ., and State Key Laboratory of Ocean Engineering, Shanghai 200240, China. E-mail: wzhf_x@163.com

[3]Associate Professor, Dept. of Civil Engineering, Univ. of Hong Kong, Hong Kong 999077, China. E-mail: junyang@hkucc.hku.hk

[4]Associate, Arup, 77 Water St., New York, NY 10005. E-mail: chu.ho@arup.com

Note. This manuscript was submitted on August 15, 2012; approved on March 20, 2013; published online on March 22, 2013. Discussion period open until May 1, 2014; separate discussions must be submitted for individual papers. This paper is part of the ***Journal of Geotechnical and Geoenvironmental Engineering***, Vol. 139, No. 12, December 1, 2013. ©ASCE, ISSN 1090-0241/2013/12-2060–2069/$25.00.

Review of Existing Methods

The existing methods for estimating jet grout column diameter are either based on an empirical approach or a theoretical approach. In this study, the existing methods including the empirical approach [Eqs. (1) (Shibazaki 2003) and (2) (Mihalis et al. 2004)] and the theoretical approach [Eqs. (3) (Modoni et al. 2006) and (4) (Ho 2007)] are listed as follows:

$$D_0 = k p_g^{k_1} Q_g^{k_2} N^{k_3} V_m^{k_4} \quad (1)$$

$$D_0 = n_1 \left(p_g Q_g / v_s \right)^{n_2} \quad (2)$$

$$D_0 = 2 \int_0^{t^*} V_c t^* dt^* \quad (3)$$

$$D_0 = 12.5 d_0 \sqrt{\frac{p_g - p_0}{q_{bu}}} + D_r \quad (4)$$

where D_0 = calculated diameter of the column; p_g = jetting pressure of grout; Q_g = flow rate of grout; N = number of passes of the jet; v_m = horizontal tangential velocity of the nozzle; v_s = withdrawal rate of the rod; V_c = penetration rate of the fluid jet in soil; t^* = duration of action of the jet on soil; d_0 = nozzle diameter; p_0 = presiding pressure at nozzle outlet; q_{bu} = ultimate bearing resistance of soil; D_r = diameter of monitor; and k, k_1, k_2, k_3, k_4, n_1, and n_2 = empirical coefficients.

The empirical methods were developed based on observations derived from jet-grouting field trials and attempt to mathematically correlate column diameter to the various operational parameters using a power law. Hence, these relationships do not have a clear physical meaning (Croce and Flora 2000). In the empirical methods, only certain operational parameters, such as jetting pressure, flow rate, and withdrawal rate of the nozzle, have been considered, while other important parameters, such as nozzle diameter, effect of air shroud in double and triple fluid systems, rotation speed, grout characteristics, and soil properties, have been ignored. The empirical coefficients were derived for specific ground conditions, and it would be difficult to apply them for other jet-grouting projects in which the ground conditions are different.

The theoretical methods were based on theories of turbulent flow and soil erosion (Modoni et al. 2006; Ho 2007). With these methods, the physical process of jet grouting, i.e., the interaction between fluid jet and soils, can be reasonably described. Modoni et al. (2006) presented two models for describing the physical process of jet grouting in different soils: a seepage model for gravelly soils and an erosion model both for sandy soils and clayey soils. For the very pervious soils (gravels and sandy gravels), Modoni et al. (2006) presented a seepage model to simulate the phenomenon of soil pore filling by an injected fluid. In the erosion models for sandy and clayey soils, the rate of penetration of the fluid jet in the soil and the duration of jetting action are considered to be important factors governing the achievable column diameter. In the derivation of the penetration rate and duration of jetting action, variables such as fluid properties, flow rate, withdrawal rate, nozzle diameter, and number of nozzles as well as soil resistance have been considered; however, the effect of compressed air, rotation speed, and particle size distribution have been neglected.

Ho (2007) presented a simplified method to estimate the column diameter, which accounted for several important parameters, such as jetting pressure, nozzle diameter, and soil-bearing resistance. The method was limited to the single fluid system and did not consider the effects of compressed air, particle size distribution, rotation speed, withdrawal rate, and grout properties.

Diameter of Jet Grout Column

In the process of jet grouting, fluids (grout or water) are jetted into the ground with high velocities (typically several hundred meters per second) from small-diameter nozzles fixed on a monitor rotating at a constant rate. The high velocity fluid jets erode the in situ soil and mix the eroded soil with grout to form a soil-cement column [Fig. 1(a)]. If the monitor is stationary with the exit nozzle velocity held constant, an ultimate erosion distance (x_L) for any given type of soil when the injection time is indefinitely long exists [Fig. 1(b)]. In actual fact, during jet grouting, the injection time would be limited by the rotation and withdrawal of the monitor, hence resulting in a shorter erosion distance. Because the diameter of a jet grout column is related to the ultimate erosion distance and injection time, in this study, an analytical equation is proposed for estimating the column diameter as follows:

$$D_0 = 2R_c = 2\eta x_L + D_r \quad (5)$$

where D_0 = calculated diameter of column; R_c = calculated radius of column; η = reduction coefficient accounting for the effect of the

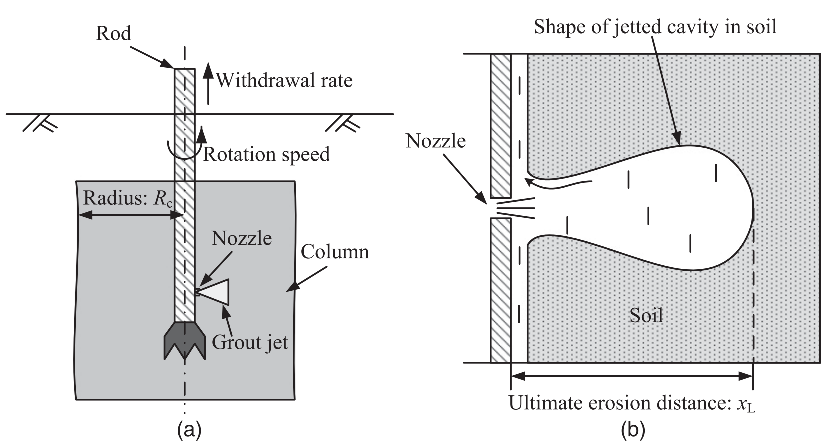

Fig. 1. Schematic view of jet grouting

J. Geotech. Geoenviron. Eng., 2013, 139(12): 2060-2069

injection time; x_L = ultimate erosion distance; and D_r = diameter of monitor. The diameters of monitors commonly adopted in the industry for single fluid, double fluid, and triple fluid systems are 60, 76, and 90 mm, respectively (Lunardi 1997). In this study, all three monitor sizes were considered in the analysis.

Ultimate Erosion Distance

In this study, the turbulent kinematic flow theory is utilized to analyze the distribution of fluid velocity after jetting out from the nozzle (Rajaratnam 1976). Using a similar approach as Modoni et al. (2006), it is assumed that the properties of the injected fluid are the same as the surrounding fluid based on the consideration that both the injected fluid and surrounding fluid are typically suspensions of cement particles, although some soil particles may also be contained in the surrounding fluid. As shown in Fig. 2, as fluid with an initial velocity of v_0 is ejected from a round nozzle, two flow regions are developed: (1) initial zone ($x \le x_0$) and (2) main zone ($x > x_0$). In the initial zone, the maximum velocity of the jet along the nozzle axis ($v_{x\max}$) remains constant and is equal to the exit nozzle velocity (v_0). In this study, the influence of the initial zone has been ignored because the range of the initial zone is very limited when the nozzle diameters are very small. Within the main zone, the maximum velocity of the jet along the nozzle axis decreases with distance from the nozzle based on the following relationship (Rajaratnam 1976):

$$\frac{v_{x\max}}{v_0} = \alpha \frac{d_0}{x}, \quad (x > x_0) \tag{6}$$

where $v_{x\max}$ = maximum velocity of the fluid along the x-direction; v_0 = exit velocity of the fluid at the outlet of the nozzle; d_0 = nozzle diameter; x = distance from the nozzle ($x > x_0$); and α = attenuation coefficient, which is related to the characteristics of the fluid.

For a given soil type, when the jets impact onto the surface of the soil, there is a minimum value of jet velocity that will initiate soil erosion, herein defined as the critical velocity (v_L). The critical velocity for soil erosion is related to the properties of the jetting fluid and erosion resistance of the soil. If the critical velocity (v_L) is set equal to the maximum velocity of the fluid along the nozzle axis in Eq. (6), the erosion distance x_L can be obtained as

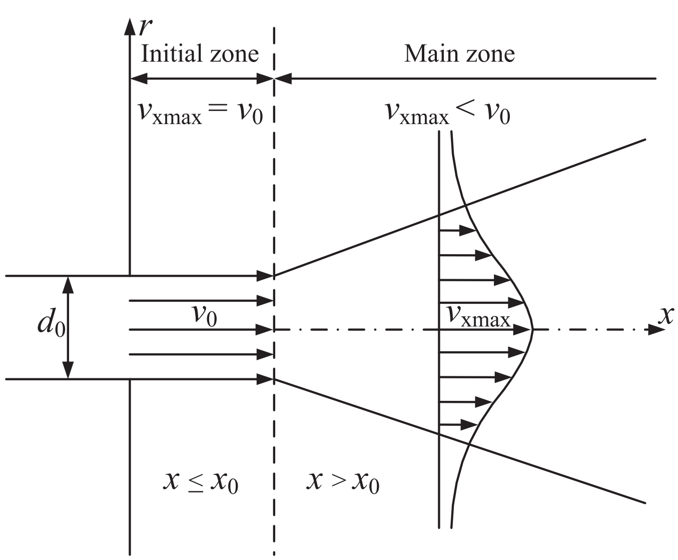

Fig. 2. Submerged free jet from a round nozzle (data from Rajaratnam 1976)

$$x_L = \frac{\alpha d_0 v_0}{v_L} \tag{7}$$

Attenuation Coefficient (α)

Conventionally, there are three primary systems used for jet grouting: (1) single fluid (grout), (2) double fluid (air and grout), and (3) triple fluid (air, grout, and water). In general, the parameter α describes the degree of attenuation of $v_{x\max}$ with distance x. When the property of fluid jet is altered, α will be different. For jet-grouting systems, water or grout is used as the jetting fluid. In the case of water jetting into a water medium, Modoni et al. (2006) evaluated the value of α_w to be approximately 16 based on the laboratory experimental data of de Vleeshauwer and Maertens (2000). Shibazaki (2003) indicated that the attenuation of fluid velocity along the jet axis is also influenced by the nozzle shape. This effect may be represented by the relationship $\alpha_w = 16A$, where A is the shape factor accounting for the effect of the nozzle shape. In this study, considering the lack of detailed information of the nozzle configuration, the value of A is assumed to be 1 for simplicity. This simplification may result in some uncertainty in the calculated results of α_w, with corresponding predicted column diameters that may be higher or lower than the actual value.

In the case of grout as the jetting fluid, the attenuation coefficient α_g can be determined by introducing a parameter B, which reflects the ratio of the properties of water and grout

$$\alpha_g = \frac{\alpha_w}{B} \tag{8}$$

Modoni et al. (2006) suggested that the parameter B can be expressed as a function of the ratio between the laminar kinematic viscosities of grout and water. The laminar kinematic viscosity is defined as the ratio between apparent laminar viscosity and density, hence

$$B = \sqrt{\frac{\mu_g/\rho_g}{\mu_w/\rho_w}} \tag{9}$$

where μ_g = apparent laminar viscosity of grout; μ_w = apparent laminar viscosity of water (0.001 Pa·s); ρ_g = density of grout; and ρ_w = density of water (1,000 kg/m^3). In this study, a correlation between apparent laminar viscosity of grout (μ_g) and water/cement ratio by weight (W/C) was derived using regression analysis based on published data (Raffle and Greenwood 1961; Chen et al. 2003; Chupin et al. 2003; Rosquoet et al. 2003), as indicated in Fig. 3 and Eq. (10). The density of grout (ρ_g) can be obtained using Eq. (11), where ρ_c and ρ_w are the density of cement and water, respectively, and W/C is the water/cement ratio of the grout admixture. The density of the cement particle may be taken as 3,150 kg/m^3

$$\mu_g = 0.007(W/C)^{-2} \tag{10}$$

$$\rho_g = \frac{\rho_w \rho_c[1 + (\mathrm{W/C})]}{\rho_w + \rho_c(\mathrm{W/C})} \tag{11}$$

As shown previously, the value of α for different jet-grouting systems may be determined as follows:

1. Single fluid system: the cutting jet consists of fluid grout, and the value of α_s varies with the water/cement ratio of the grout mix. In this study, it is assumed that

$$\alpha_s = \alpha_g \tag{12}$$

J. Geotech. Geoenviron. Eng., 2013, 139(12): 2060-2069

2. Double fluid system: the cutting jet consists of fluid grout surrounded by a compressed air shroud. The interaction between air, grout, and soil is complex; hence, for all practical purposes, the effect of compressed air is considered empirically in this study. The presence of the compressed air shroud results in an enlargement of the jet grout column diameter, and the value of α_d is greater than that in a single fluid system. Based on published literature, Fig. 4 shows a comparison of the column diameters achieved using double and single fluid systems. As can be seen, the increment of jet grout column diameter due to the influence of compressed air is from 30 to 90%. To account for the influence of the compressed air, a dimensionless parameter ψ is introduced as follows:

$$\alpha_d = \psi\alpha_g \tag{13}$$

The parameter ψ is related to the pressure of the injected air (p_a). In practice, p_a varies within a range of $0.5-1.5$ MPa (Lunardi 1997; Long 2003; Burke 2004). Within this range of p_a, it is proposed that ψ can be reasonably determined assuming a linear relation (Fig. 5)

$$\psi = 1 + 0.054\frac{p_a}{p_{\text{atm}}} \tag{14}$$

where p_a = pressure of the injected air; and p_{atm} = atmospheric pressure (100 kPa). By varying p_a between 0.5 and 1.5 MPa, the value of ψ calculated using Eq. (14) ranged from approximately 1.27 to 1.81. Hence, a 30–90% increase in column diameter is achieved with a variation of 27–81% in air pressure. Fig. 4 suggests that prediction using Eq. (14) is reasonable.

3. Triple fluid system: the cutting jet consists of water surrounded by a compressed air shroud, and α_w is equal to 16. Considering the effect of the compressed air in a similar way as for the double fluid system, α_t can be estimated using

$$\alpha_t = \psi\alpha_w \tag{15}$$

Based on the consideration that (1) interaction between air, water, and soil is highly complex and cannot be explained explicitly at present; (2) experimental data for clarifying the difference in behavior of a water jet with and without an air shroud is very limited; and (3) experimental data for clarifying the difference in behavior of an air-shrouded water jet and an air-shrouded grout jet is also very limited, adopting Eq. (14) as a first-order approximation for the air-shrouded water jet was considered reasonable.

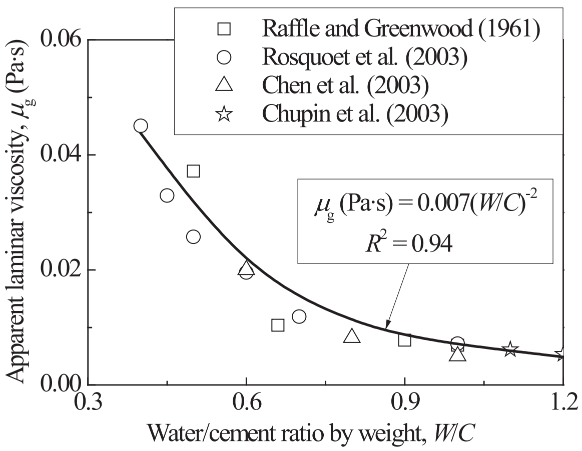

Fig. 3. Variation of apparent laminar viscosity of grout with water-cement ratio of grout admixture

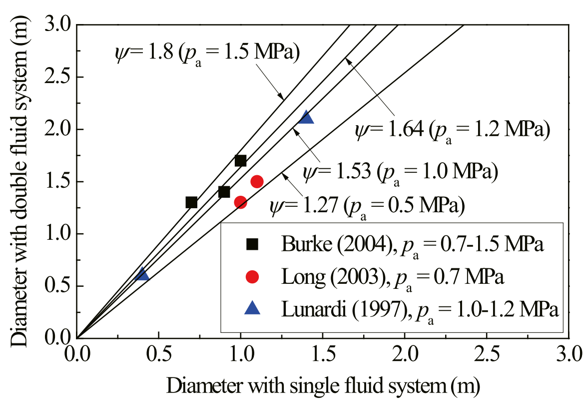

Fig. 4. Comparison of column diameters formed using double fluid and single fluid systems

Critical Velocity

Dabbagh et al. (2002) studied the erosion of soil particles by a continuous water jet using laboratory tests, and proposed the following empirical equation for estimating the critical velocity for soil erosion:

$$v_L = \beta\left(\frac{q_u}{p_{\text{atm}}}\right)^k \tag{16}$$

where q_u = erosion resistance of soil; p_{atm} = atmospheric pressure (100 kPa); β = characteristic velocity with a value equal to the critical velocity when the soil resistance is equal to the atmospheric pressure; and k = dimensionless exponent, with a proposed value of 0.5 based on the laboratory test results and the work of other researchers (Farmer and Attewell 1964).

The characteristic velocity (β) is influenced by the particle size distribution of the soil. Experimental results from Dabbagh et al. (2002) indicate that the characteristic velocity (β) in fine-grained soils increases with increasing content of fine particles less than 75 μm in size (M_c). Field experience involving jet grouting in

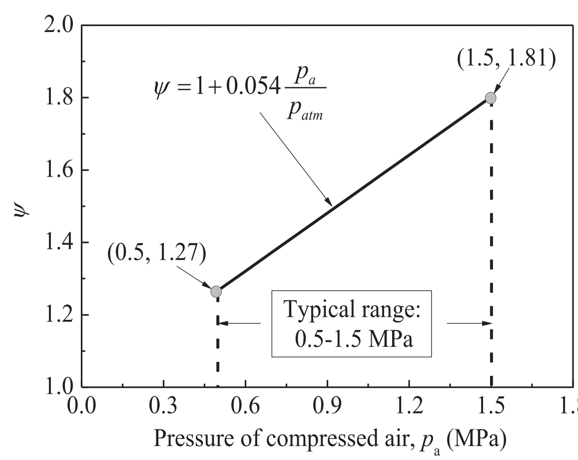

Fig. 5. Variation of dimensionless parameter ψ with pressure of injected compressed air

J. Geotech. Geoenviron. Eng., 2013, 139(12): 2060-2069

different soils also shows that for the same operational parameters and soil strength, the smaller the soil particles, the smaller the achievable column diameter. However, there is currently no meaningful expression for β in terms of particle size distribution. In this study, the content of fine particles less than 75 μm in size (M_c) and the average size of the soil particle (D_{50}) were adopted as parameters representing the influence of particle size distribution on the characteristic velocity (β). In addition, considering that the influence of M_c on β may not be significant for clean sands, a piecewise function was formulated using $M_c = 5\%$ as the criterion, which is the maximum content of fine particles in clean sands based on the Unified Soil Classification System (ASTM 2000). Thus, β can be expressed as a function of M_c and D_{50} as follows:

$$\beta = \begin{cases} b_0 \cdot \left(\frac{M_c}{100}\right)^{b_1} \left(\frac{D_{50}}{D_f}\right)^{b_2}, & 5 \le M_c \le 100 \\ b_0 \cdot \left(\frac{5}{100}\right)^{b_1} \left(\frac{D_{50}}{D_f}\right)^{b_2}, & 0 \le M_c \le 5 \end{cases} \quad (17)$$

where M_c = content of fine particles less than 75 μm in size as a percentage; D_{50} = average size of the soil particle in millimeters; and D_f = size of No. 200 sieve (0.075 mm). The characteristic velocity (β) in Eq. (17) is expressed in meters per second. The regression constants $b_0 = 2.87$, $b_1 = 0.4$, and $b_2 = -0.4$ are obtained by fitting the measured values of β reported by Dabbagh et al. (2002), as shown in Fig. 6.

For each soil type, the approach for determining the erosion resistance (q_u) in Eq. (16) may be different:

1. For clayey soils, $q_u = 2c_u$, where c_u = undrained shear strength; and
2. For sandy soils, $q_u = 2\tau_f$, where τ_f = shear strength of sand and $\tau_f = c' + \sigma' \tan\phi', \sigma'$ = normal effective stress, c' = effective cohesion, and ϕ' = effective friction angle.

Based on Eqs. (16) and (17), it can be deduced that a larger critical velocity is necessary to initiate erosion when the soil strength is higher or when the particle size of the soil is smaller (Fig. 7). The critical velocity can be used as an indicator for the erodibility of a soil, where a smaller critical velocity would indicate a more erodible soil. Eqs. (16) and (17) are in good agreement with field observations that high plasticity clays with significant cohesion are more difficult to erode than granular soils (Burke 2004).

Exit Velocity

The exit velocity of a fluid jet at the nozzle (v_0) is related to the flow rate of the injected fluid (Q), nozzle diameter (d_0), and number of nozzles (M). Based on the continuity of flow in the monitor, the exit velocity (v_0) can be obtained as

$$v_0 = \frac{4Q}{M\pi d_0^2} \quad (18)$$

where Q = flow rate of the fluid; and M = number of nozzles on the monitor.

Reduction Coefficient for Erosion Distance

The erosion distance that can be achieved varies with injection time and can reach the ultimate erosion distance (x_L) if the injection time is sufficiently long. However, in actual practice, the injection time depends on the horizontal tangential velocity of the nozzle (v_m) and the number of passes of the jet (N). The higher the horizontal tangential velocity of the nozzle (v_m), the shorter the injection time, and hence the smaller the column diameter (D_0). Similarly, the greater the number of passes of the jet (N), the greater the opportunity for the soil to be exposed to the jet, and hence the larger the column diameter (D_0). At present, there is no clear formulation relating the injection time to v_m and N. In this study, a reduction coefficient (η) has been applied to the ultimate erosion distance (x_L), as shown in Eq. (5), to account for the effect of injection time on the ultimate erosion distance. The reduction coefficient η is expressed as an empirical function of v_m and N as follows:

$$\eta = a_0 \left(\frac{v_{m0}}{v_m}\right)^{a_1} N^{a_2} \quad (19)$$

where v_m = horizontal tangential velocity of the nozzle, which is governed by the withdrawal rate v_s and rotation speed of the rod R_s, as shown in Eq. (20) proposed by Yoshida et al. (1991); N = number of passes of the jet, which is determined by the number of nozzles on the monitor M, the rotation speed R_s, and the withdrawal rate of the rod v_s and the lift step, where ΔS_t is taken as 5 cm in this study, which is a typical value in practice, as shown in Eq. (21) proposed by Yoshida et al. (1991); a_0 = correction factor corresponding to the horizontal tangential velocity of the nozzle $v_{m0} = 0.071$ m/s, which is calculated based on $R_s = 15$ rpm, $v_s = 30$ cm/min, and $D_r = 90$ mm; and a_1 and a_2 = empirical parameters

$$v_m = \sqrt{(\pi R_s D_r)^2 + v_s^2} \quad (20)$$

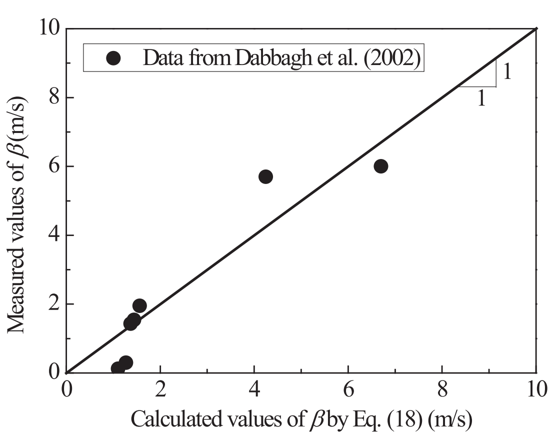

Fig. 6. Comparison of measured and calculated values of β

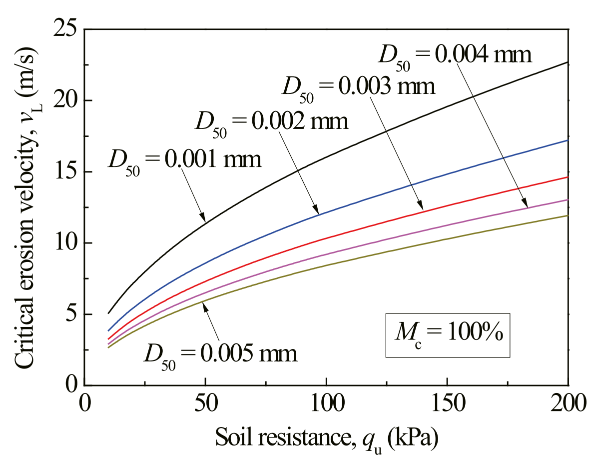

Fig. 7. Variation of critical velocity (v_L) with erosion resistance of soil (q_u)

J. Geotech. Geoenviron. Eng., 2013, 139(12): 2060-2069

$$N = M \frac{R_s}{v_s} \Delta S_t \tag{21}$$

Based on a series of laboratory tests for soft soil cutting by water jets, Yoshida et al. (1991) indicated that the value of a_1 and a_2 was approximately 0.14 and 0.2, respectively. A value of $a_0 = 0.09$ was obtained in this study based on curve fitting the field data reported by Croce and Flora (1998), Durgunoglu et al. (2003), and Nikbakhtan and Osanloo (2009). The correction factor a_0 varies with v_{m0} so that a_0 and v_{m0} must be defined as a pair.

From Eqs. (5) and (19), it can be seen that for a given D_r, x_L, and R_s, a different withdrawal rate (v_s) produces a different reduction coefficient (η), which will result in a different column diameter (D_0). Fig. 8 shows the normalized relationship between the reduction coefficient (η) and withdrawal rate (v_s), where v_{s0} is taken as 30 cm/min and $\eta_0 = 0.06$ is calculated using $R_s = 15$ rpm, $v_s = 30$ cm/min, $D_r = 90$ mm, $M = 1$, and $\Delta S_t = 5$ cm. Based on the field trial data reported by Malinin et al. (2010) involving the investigation of withdrawal rate on column diameter for different rotation speeds, it can be seen that the empirical relationship given by Eq. (19) is in reasonable agreement with the field results. Fig. 8 also shows that for a given withdrawal rate (v_s), the value of η changes very little with variation in rotation speed (R_s). The value of η calculated by varying R_s between 5 and 30 rpm differs only by approximately 10%. This is consistent with the common practice in jet grouting of increasing rotation speed to improve the uniformity of columns but not to enlarge the column diameter.

Application to Case Histories with Different Jet-Grouting Systems

The proposed method is applied to four case histories from published literature:

1. Case A: Croce and Flora (1998) presented a case history of the single fluid system, which involved a field test of seven jet grout columns at a depth of 10 m in a deposit of pyroclastic silty sand. The test site is located at the foothill of Mount Vesuvius, near Naples, Italy. The mean value of the friction angle ϕ' and cohesion c', derived from drained triaxial tests, was approximately 35° and 55 kPa, respectively. The unit weight of soil γ_s was approximately 18 kN/m^3. The content of fine particles less than 75 μm in size ranged from 10 to 30%. The average size of the soil particles (D_{50}) was approximately 0.112 mm.
2. Case B: Durgunoglu et al. (2003) reported a jet-grouting field trial using a double fluid system located in Izmir, Turkey. Four jet grout columns were installed to investigate the effect of operational parameters on the diameter and uniformity of the column in this field trial. The undrained shear strength and the fines content of the soil were approximately 50 kPa and 35%, respectively. The average size of the soil particles (D_{50}) was approximately 0.080 mm.
3. Case C: Nikbakhtan and Osanloo (2009) reported a case history involving the field trial of six jet grout columns in clay conducted at the Shahriar Dam in Iran. The jet grouting columns in this field trial were formed by using a triple fluid system. The purpose of the trial was to obtain the most appropriate operational parameters for jet grouting of the soils. The unconfined compressive strength, liquid limit, and plasticity index of the in situ soils were assessed to be 50 kPa, 45%, and 20, respectively. The fines content of the soils and average size of the soil particles (D_{50}) were approximately 90% and 0.023 mm, respectively.
4. Case D: Shen et al. (2009b) described a field test located along the west bank of the Huangpu River in Shanghai, China, for confirming the efficacy of an enhanced triple fluid system. By allowing the soils to be cut twice, first by the upper water jet and then by the lower grout jet, much larger column diameters can be achieved. Three test columns 40 m in length (C1, C2, and C3) were installed using the enhanced triple fluid system in the field trial (Fig. 9). Fig. 10 shows the geotechnical profile and soil properties at the test site. The subsoil profile was generally stratified and consisted of backfill from 0.0 to 7.6 m, clayey silt from 7.6 to 15.6 m, soft clay from 15.6 to 25.4 m, stiff silty clay from 25.4 to 29.6 m, sandy silt from 29.6 to 37.5 m, and silty sand below a depth of 37.5 m. More details on the soil properties can be found in previous publications (Xu et al. 2009; Shen and Xu 2011; Tan and Wei 2012). The natural water content of these soils ranged from 20 to 50%, and the unit weight of soils ranged from 16.9 to 19 kNm^3. The undrained shear strength (c_u) and drained friction angle (ϕ') were determined from the standard penetration test (SPT) blow counts using Eqs. (22) (Stroud 1974) and (23) (Hatanaka and Uchida 1996)

$$c_u(\text{kPa}) = (4.4 \text{ to } 6)N_{\text{SPT}} \tag{22}$$

$$\phi'(°) = \sqrt{20\frac{N_{\text{SPT}}}{\sqrt{\sigma'_v/98}}} + 20 \tag{23}$$

where σ'_v = effective overburden pressure expressed in kilopascals. Fig. 11 shows the particle size distribution at the test site, which indicates that the content of fine particle less than 75 μm in size is approximately 91.5, 99, 98, 54.6, and 29.2% for clayey silt, soft clay, stiff silty clay, sandy silt, and silty sand, respectively. Fig. 12 shows the column diameters of test columns measured at the different depths after excavation.

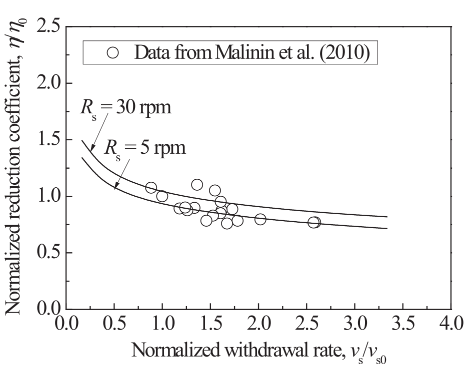

Fig. 8. Normalized relationship between reduction coefficient (η) and withdrawal rate (v_s)

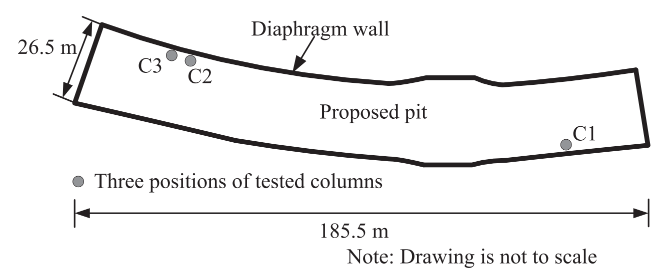

Fig. 9. Layout of three positions of test columns in Case D (data from Shen et al. 2009b)

J. Geotech. Geoenviron. Eng., 2013, 139(12): 2060-2069

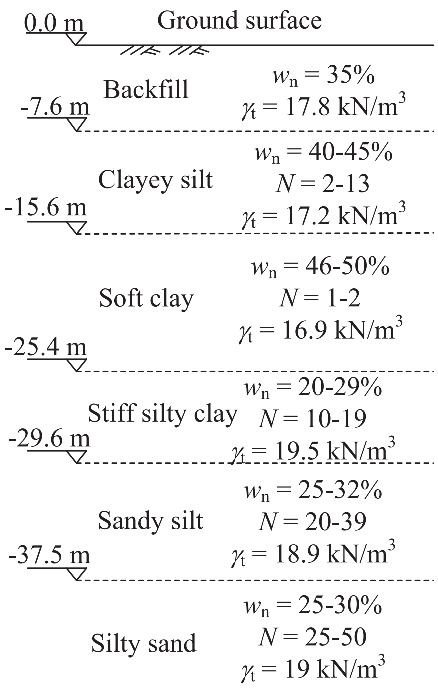

Fig. 10. Geotechnical profile and soil properties in Case D

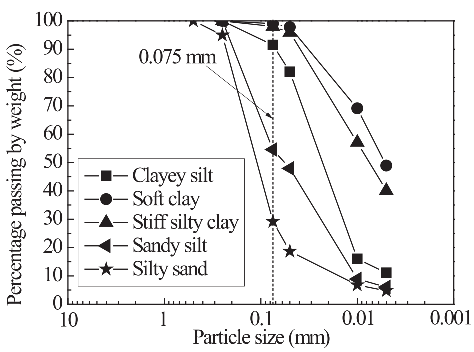

Fig. 11. Particle-size distribution of soils in Case D

Table 1 summarizes the jet-grouting parameters and average measured diameters of Cases A, B, and C for conventional jet grouting using single, double, and triple fluid systems, respectively. Predictions of column diameters were made using the relationships developed in this paper, and Fig. 13 compares the results for these three cases. As can be seen, the calculated and measured results are in good agreement.

In the case of the enhanced triple fluid system, the soil is first cut by the upper water jet and then by the lower grout jet during withdrawal of the rod. The calculation of the column diameter can be carried out in two stages. The column diameter (D_{w0}) achieved with the water jet is first calculated using the proposed method in this study followed by the determination of the additional erosion distance (L_g) achieved with the grout jet. A parameter, F, defined as the ratio of L_g to D_{w0}, is introduced for evaluating the additional effect of the grout jet. The column diameters for the enhanced triple fluid system are therefore expressed as follows:

$$D_0 = D_{w0} + L_g = (1 + F)D_{w0} \tag{24}$$

Table 2 summarizes the jet parameters for three test columns using the enhanced triple fluid system in Case D (Shen et al. 2009b).

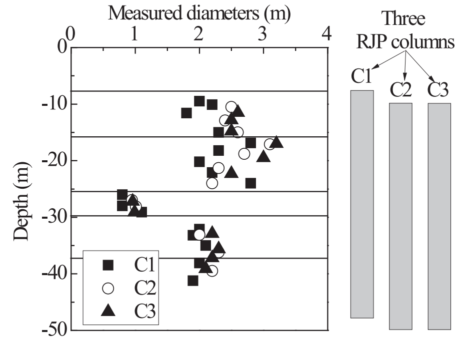

Fig. 12. Measured diameters for test columns in Case D (data from Shen et al. 2009b)

Fig. 14 shows a comparison of the calculated and measured diameters. As can be seen, the value of F varied between 0 and 0.81, with an average value of approximately 0.36. This implies that in comparison with the conventional triple fluid system, the column diameter obtained using the enhanced triple fluid system may be substantially increased in some cases or may not be increased at all in others.

Conclusions

This paper presents a generalized approach for predicting the diameter of jet grout columns based on the theoretical framework of turbulent kinematic flow and soil erosion. Based on the results of this study, the following concluding remarks are presented:

1. The proposed calculation method is a semitheoretical approach, in which the basic theoretical framework is turbulent kinematic flow and soil erosion, with some parameters determined empirically. The method is applicable to all jet-grouting systems, including the application of a compressed air shroud.
2. The proposed method takes into account all the operational parameters including the number of nozzles, diameter of nozzles, flow rate of injected fluids, properties of injected fluids, rotation speed, and withdrawal rate, as well as the soil properties, i.e., soil resistance and particle size distribution.
3. It was demonstrated that the presence of a compressed air shroud in double and triple fluid systems could enhance the diameter of jet grout columns by approximately 27–81% for the typical air pressure range of 0.5–1.5 MPa. In the case of the enhanced triple fluid system, the secondary cutting action of the high-pressure grout jet can increase the jet grout column diameter further by 36% on average.
4. The proposed method provides a means for evaluating soil erodibility in a quantitative manner by incorporating the effects of soil resistance and particle size distribution. It was shown that soils with higher strength or smaller particle size are associated with a higher critical velocity and are more difficult to erode.
5. The new equations presented account for the effect of injection time on erosion distance. It was shown that the influence of rotation speed on jet grout column diameter was not significant, which was consistent with field experience that increasing the rotation speed only improves the uniformity of column in situ soil mixing but not the diameter.
6. The proposed method was applied to four case histories involving different jet-grouting systems: single fluid, double fluid, triple fluid, and an enhanced triple fluid system. Comparison between calculated and measured diameters indicated

J. Geotech. Geoenviron. Eng., 2013, 139(12): 2060-2069

Table 1. Jet-Grouting Parameters and Measured Column Diameters from Field Trials Using Conventional Single, Double, and Triple Fluid Systems

Case	Column number	Operational parameters										Measured average diameter (m)
		M	d_0 (10^{-3} m)	p_g (MPa)	Q_g (10^{-3} m^3/s)	W/C	p_a (MPa)	p_w (MPa)	Q_w (10^{-3} m^3/s)	R_s (rpm)	v_s (10^{-3} m/s)	
A (single fluid system)[a]	1	2	2.0	45	1.38	1	—	—	—	15	5.71	0.66
	2	1	3.8	45	2.5	1	—	—	—	7.5	5.0	0.96
	3	2	2.6	45	2.35	1	—	—	—	15	6.67	0.75
	4	1	3.8	45	2.5	1	—	—	—	11	5.0	0.97
	5	2	2.6	45	2.35	1	—	—	—	10	6.67	0.71
	6	1	3.8	45	2.5	1	—	—	—	6	4.0	1.11
	7	1	3.8	45	2.5	1	—	—	—	9	4.0	0.95
B (double fluid system)[b]	1	2	2.5	40	2.25	1	1	—	—	20	11.2	0.95
	2	2	2.5	45	2.29	1.2	1	—	—	20	10.5	1.1
	3	2	2.5	40	2.19	1	1	—	—	20	9.33	1.05
	4	2	2.5	40	2.25	1	1	—	—	20	11.2	1.1
C (triple fluid system)[c]	1	2	1.7	0.3–0.5	1.33	1	0.7	35	1.07	7.5	1.25	1.15
	2	2	1.7	0.4–0.5	2.08	1	0.7	40	1.2	5	0.83	1.35
	3	2	1.7	1.5–2.0	1.75	0.7	0.7	40	1.25	5	0.83	1.03
	4	2	1.7	0.8–1.5	2.17	1	0.7	40	1.33	7	1.17	1.47
	5	2	1.7	1.5–1.6	2.5	1	0.7	35	1.13	5	0.83	1.23
	6	2	1.7	0.3–0.6	1.5	1	0.7	40	1.25	7.5	1.25	1.09

Note: A = Vesuvius, Italy; B = Izmir, Turkey; C = Shahriar Dam, Iran; d_0 = diameter of nozzles; M = number of nozzles; p_a = air pressure; p_g = grout pressure; p_w = water pressure; Q_g = flow rate of grout; Q_w = flow rate of water; R_s = rotation speed; v_s = withdrawal rate of monitor; W/C = water/cement ratio by weight.
[a]Croce and Flora (1998).
[b]Durgunoglu et al. (2003).
[c]Nikbakhtan and Osanloo (2009).

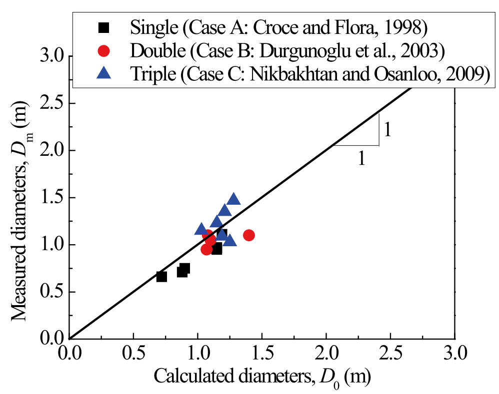

Fig. 13. Comparison of measured and calculated diameters for three different jet-grouting systems (Cases A, B, and C)

Table 2. Jet-Grouting Parameters Used in Case D

Operational parameters	Range		
	C1	C2	C3
p_w (MPa)	35	35	38
Q_w (L/min)	75	75	75
p_a (MPa)	0.5	0.6	0.7
W/C (0–30 m deep)		1:1	
W/C(> 30 m)		0.9:1	
p_g (MPa)	20	30	40
Q_g (L/min) (0–30 m deep)	80	90	95
Q_g (L/min)(> 30 m)	70	90	80
M	2	2	2
v_s (cm/min) (0–30 m deep)	4.0	5.0	6.0
v_s(cm/min)(> 30 m)	4.0	4.5	5.0
R_s(rpm)	5	6	7
d_0 (mm)	1.7	1.7	1.7

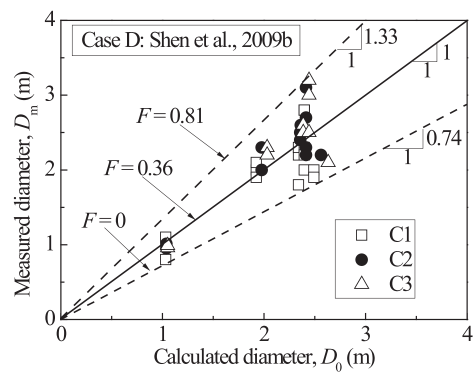

Fig. 14. Comparison of measured and calculated diameters for enhanced triple fluid system (Case D)

that the proposed method can produce a reasonable prediction of the jet grout column diameters.

Acknowledgments

The research work described herein was funded by the National Nature Science Foundation of China (NSFC) (Grant No. 41372283) and the Innovative Research Project of Shanghai Municipal Education Commission (Grant No. 13ZZ021). These financial supports are gratefully acknowledged.

Notation

The following symbols are used in this paper:

B = coefficient accounting for the difference of the characteristic between water and grout;

D_f = size of No. 200 sieve (75 μm);

J. Geotech. Geoenviron. Eng., 2013, 139(12): 2060-2069

D_r = diameter of monitor;
D_0 = calculated diameter of column;
D_{50} = average size of soil particle;
d_0 = nozzle diameter;
M = number of nozzles on the monitor;
M_c = content of particle ($< 75\ \mu$m) in soils;
N = number of passes of the jet;
p_a, p_w, p_g = jetting pressure of air, water, and grout;
p_0 = presiding pressure at nozzle outlet;
Q_g, Q_w = flow rate of grout and water;
q_{bu} = ultimate bearing resistance of soil;
q_u = erosion resistance of soil;
R_s = rotation speed of the rod;
t^* = duration of action of the jet on soil;
V_c = penetration rate of the fluid jet in soil;
v_L = critical velocity producing soil erosion;
v_m = horizontal tangential velocity of nozzle;
v_s = withdrawal rate of the rod;
$v_{x\max}$ = velocity of jetting fluid along jet axis;
v_0 = exit velocity of jetting fluid at nozzle;
x = distance from nozzle;
x_L = ultimate erosion distance;
$\alpha_s, \alpha_d, \alpha_t$ = attenuation coefficient for single, double, and triple fluid system;
α_w, α_g = attenuation coefficient for the water jet and grout jet;
β = characteristic velocity;
η = reduction coefficient on ultimate erosion distance;
μ_w, μ_g = apparent laminar viscosity of water and grout;
ρ_w, ρ_g, ρ_c = density of water, grout, and cement; and
ψ = coefficient accounting for the enhancement of jet gout column diameter due to compressed air.

References

ASTM. (2000). "Standard practice for classification of soils for engineering purposes (unified soil classification system)." *D2487*, West Conshohocken, PA.

Burke, G. K. (2004). "Jet grouting systems: Advantages and disadvantages." *GeoSupport 2004: Drilled shafts, micropiling, deep mixing, remedial methods, and specialty foundation systems*, *Geotechnical special publication 124*, J. P. Turner and P. W. Mayne, eds., ASCE, Reston, VA, 75–87.

Chai, J. C., Miura, N., and Koga, H. (2005). "Lateral displacement of ground caused by soil-cement column installation." *J. Geotech. Geoenviron. Eng.*, 131(5), 623–632.

Chen, G. X., Ji, G. J., and Huang, G. X. (2003). "Repeated joint-grouting of roller compacted concrete arc dam." *Proc., 4th Int. Symp. Roller Compacted Concrete (RCC) Dams,* A. A. Balkema, Rotterdam, Netherlands, 421–426.

Chen, J. J., Zhang, L. Y., Zhang, J. F., Zhu, Y. F., and Wang, J. H. (2013). "Field tests, modification and application of deep soil mixing method in soft clay." *J. Geotech. Geoenviron. Eng.*, 139(1), 24–34.

Chupin, O., Saiyouri, N., and Hicher, P. Y. (2003). "Numerical modeling of cement injection in saturated porous media." *Proc., 16th ASCE Engineering Mechanics Conf.,* ASCE, Reston, VA.

Croce, P., and Flora, A. (1998). "Jet-grouting effects on pyroclastic soils." *Riv. Ital. Geotec.*, 32(2), 5–14.

Croce, P., and Flora, A. (2000). "Analysis of single fluid jet-grouting." *Geotechnique*, 50(1), 739–748.

Dabbagh, A. A., Gonzalez, A. S., and Pena, A. S. (2002). "Soil erosion by a continuous water jet." *Soils Found.*, 42(5), 1–13.

de Vleeshauwer, P., and Maertens, J. (2000). "Jet grouting: State of the art in Belgium." *Proc., 4th Int. Conf. on Ground Improvement Geosystems*, Building Information Limited, Helsinki, Finland, 145–156.

Durgunoglu, H. T., et al. (2003). "A case history of ground treatment with jet grouting against liquefaction for a cigarette factory in Turkey." *Grouting and ground treatment, Geotechnical special publication 120*, L. F. Johnsen and D. A. Bruce, and M. J. Byle, eds., ASCE, Reston, VA, 452–463.

Fang, Y. S., Kao, C. C., Chain, K. F., and Wang, D. R. (2006). "Jet grouting with the superjet-midi method." *Proc. Inst. Civ. Eng. Ground Improv.*, 10(2), 69–76.

Farmer, W., and Attewell, P. B. (1964). "Rock penetration by high velocity water jet: A review of the general problem and an experimental study." *Int. J. Rock Mech. Min. Sci.*, 2(1), 135–153.

Han, J., Oztoprak, S., Parsons, R. L., and Huang, J. (2007). "Numerical analysis of foundation columns to support widening of embankments." *Comput. Geotech.*, 34(6), 435–448.

Han, J., Zhou, H. T., and Ye, F. (2002). "State of practice review of deep soil mixing techniques in China." *Transportation Research Record 1808*, Transportation Research Board, Washington, DC, 49–57.

Hatanaka, M., and Uchida, A. (1996). "Empirical correlation between penetration resistance and internal friction angle of sandy soils." *Soils Found.*, 36(4), 1–13.

Ho, C. E. (2007). "Fluid-soil interaction model for jet grouting." *Grouting for ground improvement: Innovative concepts and applications*, *Geotechnical special publication 168,* T. M. Hurley and L. F. Johnsen, eds., ASCE, Reston, VA, 1–10.

Horpibulsuk, S., Phochan, W., Suddeepong, A., Chinkulkijniwat, A., and Liu, M. D. (2012). "Strength development in blended cement admixed saline clay." *Appl. Clay Sci.*, 55, 44–52.

Long, G. Y. (2003). "Approach to factors determining the diameter of rotating spraying piles." *Geol. Chem. Miner.*, 25(3), 247–250 (in Chinese).

Lunardi, P. (1997). "Ground improvement by means of jet grouting." *Proc. Inst. Civ. Eng. Ground Improv.*, 1(2), 65–85.

Malinin, A., Gladkov, I., and Malinin, D. (2010). "Experimental research of jet grouting parameters in different soil conditions." *Geotechnical Special Publication GeoShanghai 2010: Deep and underground excavations*, Geotechnical special publication 206, F. Tonon, X. Liu, and W. Wu, eds., ASCE, Reston, VA, 49–54.

Mihalis, I. K., Tsiambaos, G., and Anagnostopoulos, A. (2004). "Jet grouting applications in soft rocks: The Athens Metro case." *Proc. Inst. Civ. Eng. Geotech. Eng.*, 157(4), 219–228.

Modoni, G., Croce, P., and Mongiovi, L. (2006). "Theoretical modelling of jet grouting." *Geotechnique*, 56(5), 335–347.

Nikbakhtan, B., and Osanloo, M. (2009). "Effect of grout pressure and grout flow on soil physical and mechanical properties in jet grouting operations." *Int. J. Rock Mech. Min. Sci.*, 46(3), 498–505.

Raffle, J. F., and Greenwood, D. A. (1961). "The relationship between the rheological characteristics of grouts and their capacity to permeate soils." *Proc., 5th Int. Conf. on Soil Mechanics and Foundation Engineering*, Dunod, Paris, 789–793.

Rajaratnam, N. (1976). *Turbulent jets*, Elsevier, Amsterdam, Netherlands.

Rosquoet, F., Alexis, A., Khelidj, A., and Phelipot, A. (2003). "Experimental study of cement grout: Rheological behavior and sedimentation." *Cement Concr. Res.*, 33(5), 713–722.

Shen, S. L., Han, J., and Du, Y. J. (2008). "Deep mixing induced property changes in surrounding sensitive marine clays." *J. Geotech. Geoenviron. Eng.*, 134(6), 845–854.

Shen, S. L., Luo, C. Y., Bai, Y., Kim, Y. H., and Peng, S. J. (2009a). "Instant solidification of soft ground horizontally using jet-grouting." *Contemporary topics in ground modification, problem soils, and geo-support*, *Geotechnical special publication 187*, M. Iskander, D. F. Laefer, and M. H. Hussein, eds., ASCE, Reston, VA, 257–264.

Shen, S. L., Luo, C. Y., Xiao, X. C., and Wang, J. L. (2009b). "Improvement efficacy of RJP method in Shanghai soft deposit." *Advances in ground improvement: Research to practice in the United States and China*, *Geotechnical special publication 188*, J. Han, G. Zheng, V. R. Schaefer, and M. Huang, eds., ASCE, Reston, VA, 170–178.

Shen, S. L., Wang, Z. F., Horpibulsuk, S., and Kim, Y. H. (2013a). "Jet-grouting with a newly developed technology: Twin-jet method." *Eng. Geol.*, 152(1), 87–95.

Shen, S. L., Wang, Z. F., Sun, W. J., Wang, L. B., and Horpibulsuk, S. (2013b). "A field trial of horizontal jet grouting with composite-pipe method in soft deposit of Shanghai." *Tunnelling Underground Space Technol.*, 35, 142–151.

Shen, S. L., and Xu, Y. S. (2011). "Numerical evaluation of land subsidence induced by groundwater pumping in Shanghai." *Can. Geotech. J.*, 48(9), 1378–1392.

Shibazaki, M. (2003). "State of practice of jet grouting." Grouting and ground treatment, ASCE, Reston, VA, 198–217.

Stroud, M. (1974). "The standard penetration test in insensitive clays and soft rocks." *European Symp. on Penetration Testing*, Swedish Geotechnical Society, Stockholm, Sweden.

Tan, Y., and Wei, B. (2012). "Observed behavior of a long and deep excavation constructed by cut-and-cover technique in Shanghai soft clay." *J. Geotech. Geoenviron. Eng.*, 138(1), 69–88.

Tsujita, M. (1996). "Recent soil improvement technique: RJP method and recent construction cases." *Found. Eng. Equip.*, 24(7), 73–77 (in Japanese).

Wang, Z. F., Shen, S. L., Ho, C. E., and Kim, Y. H. (2013). "Investigation of field installation effects of horizontal twin-jet grouting in Shanghai soft soil deposits." *Can. Geotech. J.*, 50(3), 288–297

Wang, Z. F., Shen, S. L., and Yang, J. (2012). "Estimation of the diameter of jet-grouted column based on turbulent kinematic flow theory." *Grouting and deep mixing 2012*, *Geotechnical special publication 228*, L. F. Johnsen, D. A. Bruce, and M. J. Byle, eds., Vol. 2, ASCE, Reston, VA, 2044–2051.

Xu, Y. S., Shen, S. L., and Du, Y. J. (2009). "Geological and hydrogeological environment in Shanghai with geohazards to construction and maintenance of infrastructures." *Eng. Geol.*, 109(3–4), 241–254.

Yin, J. H., and Fang, Z. (2006). "Physical modelling of consolidation behaviour of a composite foundation consisting of a cement-mixed soil column and untreated soft marine clay." *Geotechnique*, 56(1), 63–68.

Yoshida, H., Asano, R., Kubo, H., Jinbo, S., and Uesawa, S. (1991). "Effect of nozzle traverse rate and number of passes on cutting soil utilizing water jet for wider application." *Proc., 6th American Water Jet Conf.*, Houston, 381–392.

J. Geotech. Geoenviron. Eng., 2013, 139(12): 2060-2069